Available online at www.sciencedirect.com
ScienceDirect
Trans. Nonferrous Met. Soc. China 27(2017) 157−162
Transactions of Nonferrous Metals Society of China
www.tnmsc.cn

Viscous warm pressure bulging process of AZ31B magnesium alloy with different ellipticity dies

Tie-jun GAO, Qing LIU, Wen-zhuo ZHANG

Faculty of Aerospace Engineering, Shenyang Aerospace University, Shenyang 110136, China

Received 8 January 2016; accepted 14 June 2016

Abstract: Based on the bulging principle of different ellipticity dies, the methyl vinyl silicone rubber with excellent thermal stability and heat transfer performance was chosen as the viscous medium. The finite element analysis and experiments of viscous warm pressure bulging (VWPB) of AZ31B magnesium alloy were conducted to analyze the influence of different ellipticity dies on the formability of AZ31B magnesium alloy. At the same time, based on the grid strain rule, the forming limit diagram (FLD) of VWPB of AZ31B magnesium alloy was obtained through measuring the strain of bulging specimens. The results showed that at the temperature range of viscous medium thermal stability, the viscous medium can fit the geometry variation of sheet and generate non-uniform pressure field, and as the die ellipticity increases, the difference value of non-uniform pressure reduces. Meanwhile, according to the FLD, the relationship between part complexity and ultimate deformation was investigated.

Key words: AZ31B magnesium alloy; viscous warm pressure bulging; formability; different ellipticity dies; forming limit diagram

1 Introduction

With the improvement of energy saving requirements and lightweight technology, the magnesium alloys are widely applied in aviation and other transportation fields owing to a desirable combination of characteristics such as high specific strength, low density and easy recovery [1−3]. Unfortunately, the plasticity of magnesium alloys is generally lower compared with steel and aluminum alloy at room temperature due to the hexagonal crystal packed crystal structure, so the applications of magnesium alloys are limited in industrial field. The formability of magnesium alloy can still be improved significantly in certain high temperature [4−8]. Therefore, the warm forming process has become an important way to realize the forming of magnesium alloy sheet metal with complex shape. ZHENG et al [9] performed the warm hydroforming process of magnesium alloy, the liquid pressure and loading speed were optimized at warm condition. The forming of magnesium alloy parts with complex shape which could not be realized at room temperature was realized through warm hydroforming process. The warm deep drawing experiment of AZ31 magnesium alloy square part was carried out by CHANG et al [10]. Different variation schemes of blank holder force were tested. The best scheme was that with the increasing of punch stroke, the blank holder force increased firstly and then decreased. Through adopting the best blank holder force scheme, the deep drawing depth of AZ31 magnesium alloy square part can be improved greatly. MENG et al [11] tested the limit strain of AZ31 magnesium alloy sheet at 25−230 °C through combining electromagnetic forming and warm forming. In this way, the limit strain of AZ31 magnesium alloy sheet was enhanced with the increasing of temperature. In the study by AMBROGIO et al [12], the warm incremental forming of AZ31 magnesium alloy was conducted and the process parameters were optimized through finite element analysis and experiments. The formability of AZ31 magnesium alloy was improved significantly by warm incremental forming process.

A kind of semisolid, flowable and high viscosity polymer with excellent thermal stability and heat transfer performance and certain rate sensitivity was chosen as pressure-carrying medium during viscous warm pressure bulging (VWPB) process. Compared with traditional

Foundation item: Project (51575364) supported by the National Natural Science Foundation of China; Project (2013024014) supported by the Natural Foundation of Liaoning Province, China

Corresponding author: Tie-jun GAO; Tel: +86-13504999851; E-mail: tiejun_gao@163.com

DOI: 10.1016/S1003-6326(17)60018-9

warm forming methods, viscous medium could fit the geometry variation of sheet and generate the required high pressure. The large adhesive force between sheet and viscous medium could change the strain−stress state and control the flow rule of sheet during the forming process. A non-uniform pressure field could be generated to improve the formability of specimens due to the strong strain rate sensitivity of viscous medium [13−17]. In this work, the methyl vinyl silicone rubber with excellent thermal stability and mechanical property was chosen as viscous medium during warm forming process. On this basis, the research on VWPB process of AZ31B magnesium alloy with different ellipticity dies was conducted. Then, the influence of part complexity on the deformation rule and characteristic of AZ31B magnesium alloy VWPB were observed. At the same time, the FLD of viscous warm forming of AZ31B magnesium alloy was obtained, which provided an important reference for the application of viscous warm forming technology of magnesium alloys [18−21].

2 Experimental

2.1 Experimental principle and scheme

The principle of viscous warm pressure bulging is illustrated in Fig. 1. The die, sheet, viscous medium and container were heated to setting temperature using the heater and then the temperature was maintained for 30 min to ensure the temperature stable. Finally, the piston moved upward to push the viscous medium, which caused the deformation of magnesium alloy sheet. In the experiments, the long axis lengths of ellipticity dies (L) were all 60 mm and the short axis lengths of ellipticity dies (D) were 36, 42, 48, 54 and 60 mm, respectively and then corresponding ellipticities λ ($\lambda=D/L$) were 0.6, 0.7, 0.8, 0.9 and 1.0, respectively.

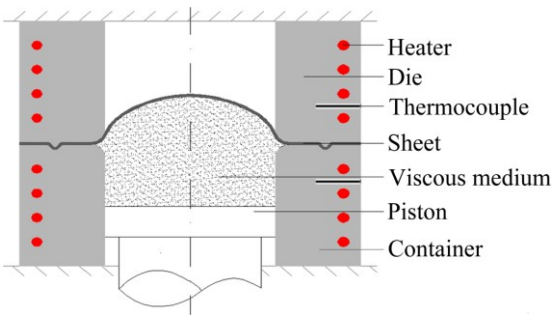

Fig. 1 VWPB principle

2.2 Property of viscous medium

Methyl vinyl silicone rubber is a kind of colorless and visco-plastic polymer which is copolymerized with dimethyl siloxane and little vinyl silicone. The methyl vinyl silicone rubber with 600000 g/mol molecular mass was chosen as viscous medium during experiments. The molecular structural formula of methyl vinyl silicone rubber is illustrated in Fig. 2. The flow and compression properties of methyl vinyl silicone rubber at different temperatures are illustrated in Fig. 3. Its bulk modulus reduced and the fluidity increased incessantly with the temperature. As the temperature exceeded 250 °C, the methyl vinyl silicone rubber decomposed into cyclic siloxane oligomer and other small molecule, then it was aged and lost elasticity.

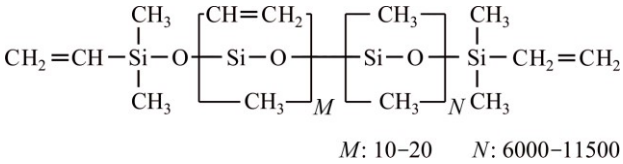

Fig. 2 Molecular structural formula of methyl vinyl silicone rubber

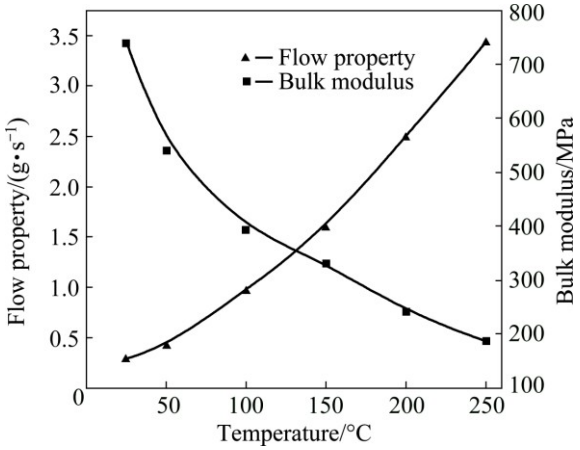

Fig. 3 Flow and compression properties of methyl vinyl silicone rubber at different temperatures

2.3 Property of AZ31B magnesium alloy

The AZ31B magnesium alloy with a thickness of 0.8 mm was annealed to relief the residual stress. Considering the thermal stability temperature range of viscous medium, the limit bulging experiments of AZ31B magnesium alloy with the speed of 0.2 mm/s were conducted at temperatures of 20, 100, 150, 200 and 250 °C in turn. The results of limit bulging experiments are shown in Fig. 4.

As the temperature increased, the limit bulging height of magnesium alloy increased, and reached the maximum at 200 °C, but it decreased at 250 °C. It was because the molecular chain of viscous medium was in active state and properties changed a lot at 250 °C, which affected the formability of magnesium alloy.

3 Finite element analysis

3.1 Finite element analysis model

In order to study the deformation rule of both

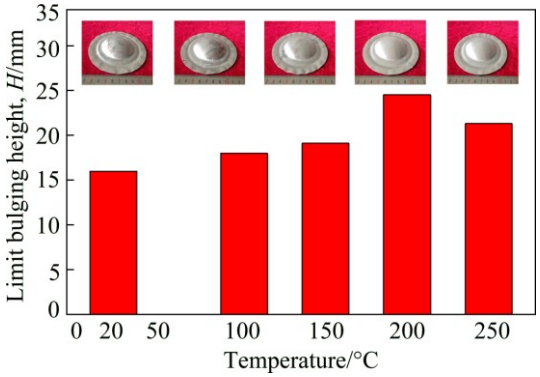

Fig. 4 Limit bulging height of specimens at different temperatures (λ=1.0)

AZ31B magnesium alloy and viscous medium, the finite element software ANSYS/LS-DYNA was used to analyze the viscous warm pressure bulging process of AZ31B magnesium alloy with different ellipticity dies. The finite element analysis (FEA) model which consisted of die, sheet, viscous medium, container and piston is illustrated in Fig. 5. The sheet, die, container and piston were meshed as No. 163 shell element and the viscous medium was meshed as No. 164 solid element. The friction coefficient between sheet and die was 0.1, the friction coefficient between viscous medium and sheet was 0.2. The properties of viscous medium and magnesium alloy are shown in Fig. 3 and Fig. 6.

3.2 Results of finite element analysis

The equivalent stress distribution of specimens

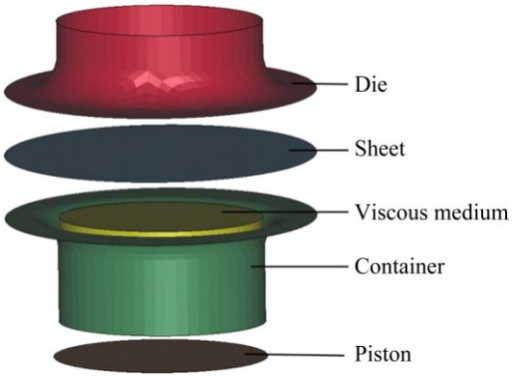

Fig. 5 FEA model (λ=0.8)

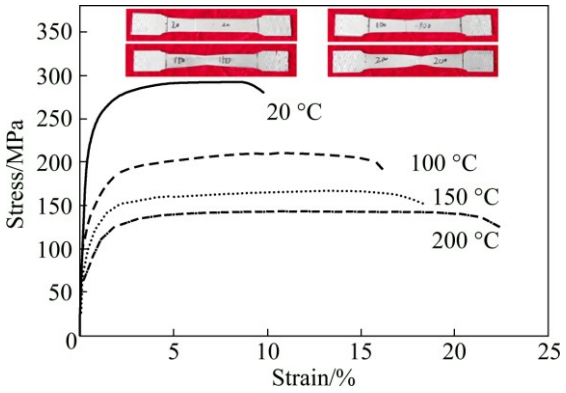

Fig. 6 Stress−strain curves of AZ31B magnesium alloy at different temperatures (0.2 mm/s)

with different ellipticity dies at bulging height H=14 mm is shown in Fig. 7. The maximum equivalent stress of specimen located at the central area. The maximum equivalent stresses with die ellipticities λ=0.6, 0.8 and 1.0 were 142.0, 133.9 and 126.6 MPa, respectively. With the increasing of die ellipticity, the maximum equivalent stress reduced. The minimum equivalent stress of specimen located at the flange area. The minimum equivalent stresses with die ellipticities λ=0.6, 0.8 and 1.0 were 79.6, 85.9 and 89.3 MPa, respectively. With the increasing of die ellipticity, the minimum equivalent stress increased and the difference value between the maximum and minimum equivalent stress reduced. This showed that with the decreasing of die ellipticity, the symmetry of specimen reduced and the complexity increased accordingly. The deformation of sheet was more difficult which was easy to fracture.

The pressure distribution of viscous medium with die ellipticities λ=0.6 and 1.0 at bulging height H=14 mm is shown in Figs. 8 and 9, respectively. During the deformation process, the pressure at specimen central area (P_1) was lower than that at the flange area (P_2), which was helpful to decrease the stress at central area and to increase the stress at flange area. So the deformation of specimen at central area could be postponed and the deformation of specimen at flange area could be promoted (shown in Fig. 10), Thereby the

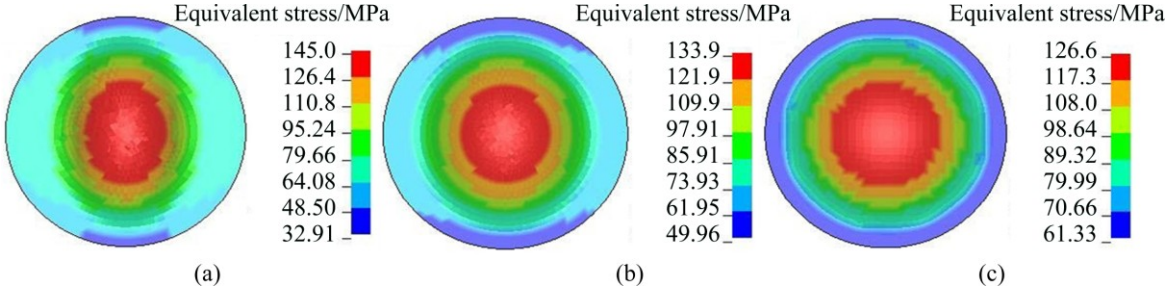

Fig. 7 Equivalent stress distribution of specimens with different ellipticity dies (H=14 mm): (a) λ=0.6; (b) λ=0.8; (c) λ=1.0

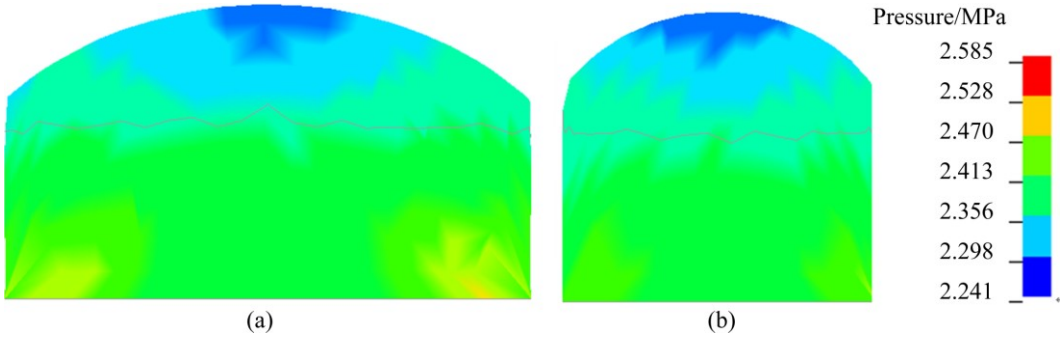

Fig. 8 Pressure distribution of viscous medium with die ellipticity λ=0.6 (H=14 mm): (a) Long axis section; (b) Short axis section

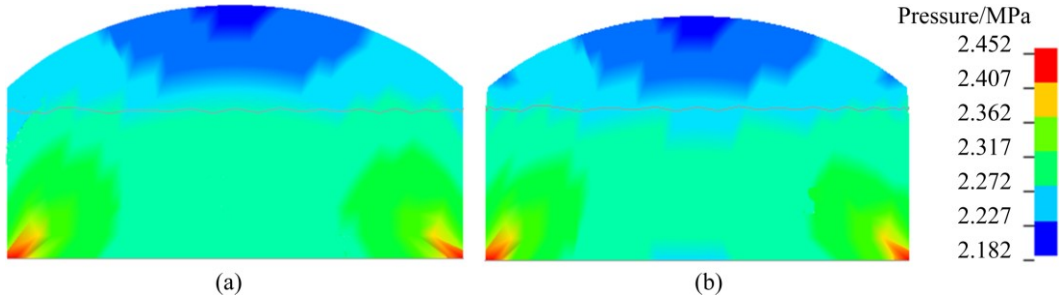

Fig. 9 Pressure distribution of viscous medium with die ellipticity λ=1.0 (H=14 mm): (a) Long axis section; (b) Short axis section

bulging formability of magnesium alloy was enhanced. The pressure difference value ($\Delta P=P_2-P_1$) of viscous medium in different ellipticity dies is shown in Fig. 11. As the ellipticity decreased, the pressure difference value increased, so the large stress at central area induced by asymmetric of bulging specimen was better relieved.

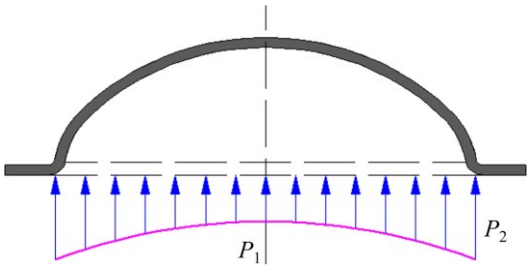

Fig. 10 Non-uniform pressure vector diagram

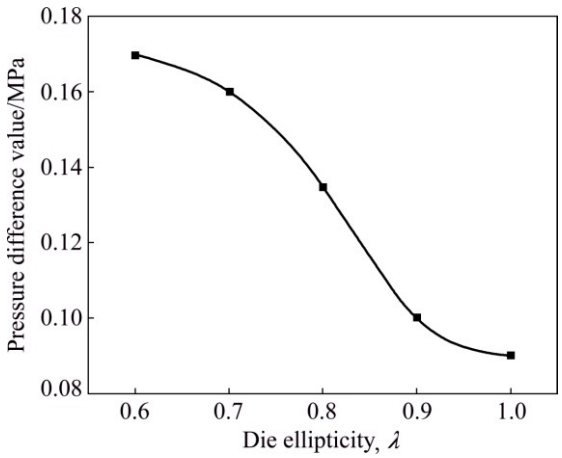

Fig. 11 Difference value of viscous medium pressure with different ellipticity dies (H=14 mm)

4 Analysis of experimental results

According to the finite element analysis results, the viscous warm pressure bulging experiments with different ellipticities were carried out. The 3 mm diameter circular grid patterns were printed on the sheet surface by PEDB-300 laser making machine before the experiment.

The wall thickness reduction rates of specimens along the long axis and short axis with different die ellipticities at bulging height H=14 mm are illustrated in Fig. 12. The maximum wall thickness reduction rates were 26.8%, 22.4% and 19.6% when λ=0.6, 0.8 and 1.0, respectively. With the die ellipticity increased, the wall thickness distribution became more uniform. The experimental results were basically tallies with the finite element analysis results. The limit bulging heights in different die ellipticities at 200 °C are shown in Fig. 13. As the die ellipticity decreased, the symmetry of specimen decreased and the complexity increased gradually. Meanwhile, the equivalent stress of specimen increased (shown in Fig. 7) which was easy to fracture, so the limit bulging height decreased.

As shown in Fig. 14, the AZ31B magnesium alloy VWPB FLD was obtained through measuring grid strain of limit bulging specimens at different temperatures. When the temperature was below 100 °C, the plasticity of magnesium alloy was in a low state, which led to fracture at the die throat. Thus only the FLD at 150 °C and 200 °C was graphed. Compared with 150 °C, the maximum and minimum of major strain (ε_1) and minor strain (ε_2) at 200 °C show remarkable increasing.

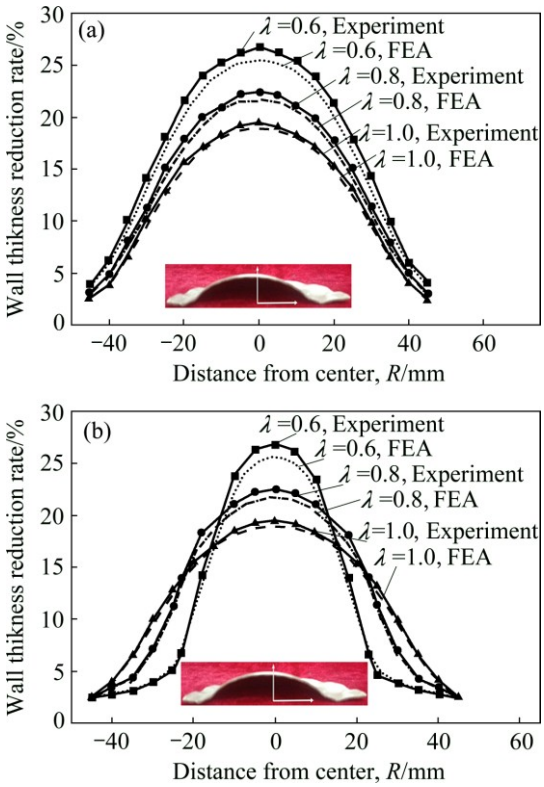

Fig. 12 Wall thickness reduction rates of specimens with different ellipticity dies (H=14 mm): (a) Long axis direction; (b) Short axis direction

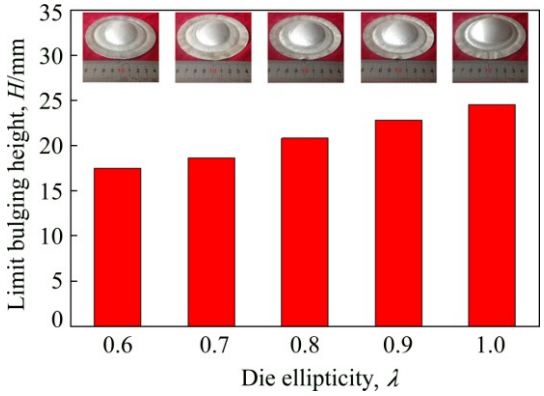

Fig. 13 Limit bulging height of specimens with different die ellipticities

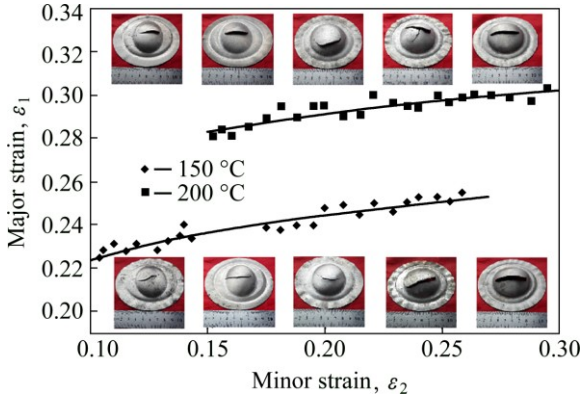

Fig. 14 Forming limit diagram

5 Conclusions

1) The optimized viscous warm bulging temperature for magnesium alloy is 200 °C. As the temperature exceeds 250 °C, the physical properties of viscous medium change greatly, which have great influences on the formability of magnesium alloy.

2) Viscous medium can maintain great rate sensitive at high temperature, and generates non-uniform pressure field which is helpful to enhance the deformation of material.

3) The difference value of non-uniform pressure of warm viscous medium is related to the die ellipticity. Generally, as the die ellipticity increases, the difference value of non-uniform pressure increases, which is helpful to improve the formability of magnesium alloy.

4) The VWPB FLD of AZ31B magnesium alloy was established by conducting limit bulging experiments with different ellipticity dies. The relationship between part complexity and ultimate deformation is investigated, which provides a reference for the research on the deformation property of magnesium alloy.

References

[1] CHAN L C, LU X Z. Material sentivity and formability prediction of warm-forming magnesium alloy sheets with experimental vertification [J]. The International Journal of Advanced Manufacturing Technology, 2014, 71(1): 253−262.

[2] LEE Y S, KIM M C, KIM S W, KWON Y N, CHOI S W, LEE J H. Experimental and analytical studies for forming limit of AZ31 alloy on warm sheet metal forming [J]. Journal of Materials Processing Technology, 2007, 187−188: 103−107.

[3] LIU Di, LIU Zu-yan, WANG Er-de. Evolution of twins and texture and its effects on mechanical properties of AZ31 magnesium alloy sheets under different rolling process parameters [J]. Transactions of Nonferrous Metals Society of China, 2015, 25(11): 3585−3594.

[4] WANG Lei, QIAO Qi, LIU Yang, SONG Xiu. Formability of AZ31 Mg alloy sheets within medium temperatures [J]. Journal of Magnesium and Alloys, 2013, 1(4): 312−317.

[5] AGNEW S R, DUYGULU Ö. Plastic anisotropy and the role of non-basal slip in magnesium alloy AZ31B [J]. International Journal of Plasticity, 2005, 21(6): 1161−1193.

[6] MAKSOUD I A, AHMED H, RÖDEL J. Investigation of the effect of strain rate and temperature on the deformability and microstructure evolution of AZ31 magnesium alloy [J]. Materials Science and Engineering A, 2009, 504(1): 40−48.

[7] HUANG Guang-sheng, LI Hong-cheng, SONG Bo, ZHANG Lei. Tensile properties and microstructure of AZ31B magnesium alloy sheet processed by repeated unidirectional bending [J]. Transactions of Nonferrous Metals Society of China, 2010, 20(1): 28−33.

[8] HUANG Guang-sheng, ZHANG Hua, GAO Xiao-yun, SONG Bo, ZHANG Lei. Forming limit of textured AZ31B magnesium alloy sheet at different temperatures [J]. Transactions of Nonferrous Metals Society of China, 2011, 21(4): 836−843.

[9] ZHENG Wen-tao, XU Yong-chao, ZHANG Shi-hong, WANG Zhong-tang. Experimental research and FEM simulation on warm hydroforming of Mg alloy mobile phone cover [J]. Journal of

Plasticity Engineering, 2006, 13(5): 92−95. (in Chinese)
[10] CHANG Qun-feng, LI Da-yong, PENG Ying-hong, ZENG Xiao-qin. Warm deep drawing of square parts of AZ31 magnesium alloy sheet adopting variable blank holder force [J]. China Mechanical Engineering, 2006, 17(S1): 16−18. (in Chinese)
[11] MENG Zheng-hua, HUANG Shang-yu, HU Jian-hua, HU Ting-ting. Formability of AZ31 magnesium alloy sheet under warm and electromagnetic forming condition [J]. China Mechanical Engineering, 2011, 22(2): 239−242. (in Chinese)
[12] AMBROGIO G, FILICE L, MANCO G.L. Warm incremental forming of magnesium alloy AZ31 [J]. CIRP Annals-Manufacturing Technology, 2008, 57(1): 257−260
[13] LIU Jian-guang, PENG Qiu-cai, LIU Yan, WANG Zhong-jin. Viscous pressure bulging of aluminium alloy sheet at warm temperatures [J]. Journal of Mechanical Science and Technology, 2007, 21(10): 1505−1511.
[14] GAO Tie-jun, LIU Yang, CHEN Pen, WANG Zhong-jin. Analysis of bulging process of aluminum alloy by overlapping sheet metal and its formability [J]. Transactions of Nonferrous Metals Society of China, 2015, 25(4): 1050−1055.
[15] WANG Zhong-jin, LIU Jian-guang. Sectional finite element analysis of coupled deformation between elastoplastic sheet metal and visco-elastoplastic body [J]. ACTA Mechanica Solida Sinica, 2011, 24(2): 153−165.
[16] GAO Tie-jun, LIU Yang, WANG Zhong-jin. Viscous inner and outer pressure forming method of thin-walled tube and its application [J]. Journal of Wuhan University of Technology: Mater Sci Ed, 2015, 30(2): 404−407.
[17] LIU Jian-guang, WANG Zhong-jin. Prediction of wrinkling and fracturing in viscous pressure forming (VPF) by using the coupled deformation sectional finite element method [J]. Computational Materials Science, 2010, 48(2): 381−389.
[18] WANG Hui, ZHOU Jie, LUO Yan, TANG Peng, CHEN You-liang. Forming of ellipse heads of large-scale austenitic stainless steel pressure vessel [J]. Procedia Engineering, 2014, 81: 837−842.
[19] YUAN Shi-jian, HU Lan, HE Zhu-bin, TENG Bu-gang, WANG Zhong-ren. Research on two-step hydro-bulge forming of ellipsoidal shell with large axis length ratio [J]. Journal of Harbin Institute of Technology, 2013, 20(3): 93−98.
[20] WANG Wu-rong, HUANG Lei, TAO Kuang-heng, CHEN Shi-chao, WEI Xi-cheng. Formability and numerical simulation of AZ31B magnesium alloy sheet in warm stamping process [J]. Materials and Design, 2015, 87: 835−844.
[21] KOJIRO U. Experimental study on concrete filled elliptical/oval steel tubular stub columns under compression [J]. Thin-Walled Structures, 2014, 78: 131−137.

AZ31B 镁合金不同椭圆度凹模黏性介质温热胀形工艺

高铁军，刘 青，张文卓

沈阳航空航天大学 航空航天工程学部，沈阳 110136

摘 要：基于不同椭圆度凹模胀形原理，选择具有良好热稳定性和导热性能的甲基乙烯基硅橡胶作为黏性介质，进行 AZ31B 镁合金黏性介质温热胀形试验，并采用有限元分析软件 ANSYS/LS-DYNA 对成形过程进行分析。确定 AZ31B 镁合金黏性介质温热胀形最佳温度，以及凹模椭圆度对 AZ31B 镁合金黏性介质温热胀形变形规律的影响。同时根据网格应变原理，通过对不同椭圆度极限胀形试件的测量，绘制出 AZ31B 镁合金黏性介质温热成形极限图(FLD)。研究结果表明，在耐热温度范围内，热态黏性介质能够适应试件几何形状的变化建立非均匀压力场，非均匀压力差值随着椭圆度的增大而减小，根据极限胀形试验绘制出的成形极限图，能够综合反映出零件复杂程度与极限变形程度的关系。

关键词：AZ31B 镁合金；黏性介质温热胀形；成形性能；不同椭圆度凹模；成形极限图

(Edited by Yun-bin HE)